Mpemba effect in self-contained quantum refrigerators: accelerated cooling

Sayan Mondal and Ujjwal Sen
Harish-Chandra Research Institute, A CI of Homi Bhabha National Institute, Chhatnag Road, Jhunsi, Prayagraj 211 019, India

arXiv:2507.15811v1 [quant-ph] 21 Jul 2025

We consider the qubit-qutrit model of self-contained quantum refrigerator and observe the quantum Mpemba effect in its cooling. In this system, the qutrit acts as the refrigerator while the qubit is to be cooled. The entire system is coupled to three bosonic heat baths, due to which the dynamics of the system is governed by a Gorini-Kossakoswski-Sudarshan-Lindblad master equation. We investigate the Liouvillian that generates the dynamics of the system and find that it has a block diagonal form. The dynamics of each element of the system's density matrix can be determined by solving the dynamical equation of the corresponding block that contains it. We find that the steady state belongs to the block containing only the diagonal elements in the energy basis. We numerically solve for the steady state and investigate the steady-state cooling over a significant region of the parameter space. Moreover, we demonstrate the quantum Mpemba effect in the refrigerator: a Mpemba state obtained by applying a unitary on the equilibrium state of the system reaches the steady state faster than the equilibrium state, despite the Mpemba state being initially farther away from the steady state. The Mpemba state thus leads to an acceleration in cooling of the cold qubit. We also find that both local and global unitaries on the qubit-qutrit system can generate the Mpemba state. Finally, we study the effect of the qubit-qutrit couplings and the system-bath couplings on the Mpemba effect.

I. INTRODUCTION

The quantum Mpemba effect [1, 2] is an apparently counter-intuitive phenomenon where a state that is farther away from the steady state, reaches the steady state faster than some other state that was initially nearer to the steady state. In the literature, the quantum Mpemba effect is usually categorized into two branches: strong Mpemba effect in open quantum systems [3, 4] and symmetry restoration in closed many-body systems [5, 6]. The latter is usually observed in quantum many-body systems where the system is initialized in a symmetry-broken state and it dynamically evolves to a state with the symmetry restored. In Ref. [5], a subsystem measure of symmetry breaking called entanglement asymmetry is introduced and it is shown that states with larger broken symmetry, restores the symmetry faster than those with lower initial symmetry breaking. This has been investigated theoretically for various models [7–9], as well as demonstrated experimentally [10]. In our work we focus on the Mpemba effect in open quantum systems.

In open quantum systems, the evolution is generated by a Liouvillian which consists of unitary part due to the system Hamiltonian as well as the dissipative part due to coupling with the environment. The Liouvillian's eigenvalue with the largest but negative real part determines the time it takes for the system to reach the steady state, and thus the corresponding right eigenvector gives the slowest decaying mode of the Liouvillian. To obtain the quantum Mpemba effect, an initial state is considered with suppressed amplitude for the slowest decaying mode, so that the time required by the state to reach steady state reduces. The effect has been studied in quantum dot systems [11–14], few-level systems [15–20], quantum harmonic oscillators [21], Dicke model [3], spin models [22, 23], bosonic systems [24, 25], Photonic systems [26] etc., and has also been demonstrated in experiments [27, 28]. In addition to these, the thermodynamics of quantum Mpemba effect [29] and its information-geometric analysis [30] has be considered. Furthermore, the effect has been investigated in systems with non-Markovian baths [31], squeezed thermal baths [32], noisy open systems [33], and initial system-environment entanglement [34].

In this work, we demonstrate the quantum Mpemba effect in the self-contained quantum refrigerator model. The quantum refrigerator [35–52] is quantum thermal machine used to cool quantum systems. They have been experimentally realized using nuclear spin systems [53] and trapped ions [54]. Quantum refrigerators can be broadly classified into two categories, measurement-based and dynamical. In the measurement-based refrigerators [55–58], the system is entangled with an auxiliary system and is cooled using measurements in the auxiliary part. Here we focus on the quantum refrigerators where cooling is achieved through dynamics [35–38]. The self-contained quantum refrigerator model, first introduced in Ref. [35], consists of two qubits, each coupled to a bath at a distinct temperatures, acting as the refrigerator. This refrigerator is coupled to the system to be cooled. It is possible to make the refrigerator smaller by considering a qutrit coupled to the two baths as the refrigerator. The model does not require any external driving and is fully autonomous.

In the qubit-qutrit model of the quantum refrigerator, initially the qubit is in equilibrium with the bath with which it is coupled to, while the qutrit is also in equilibrium with the two baths to which it is coupled to, we call this state the initial thermal state. The initial thermal state is a product state. The refrigerator dynamics begins, when the coupling between the qubit and qutrit is switched on. In order to demonstrate the Mpemba effect, we find out the slowest decaying mode of the evolution and construct a different initial state called the Mpemba state. This state is obtained by applying a unitary to the intial thermal state and it has the slowest decaying mode suppressed. We find that the in addition to global unitaries, even local ones can lead to Mpemba initial states. We also ensure that the initial Mpemba state is farther away from the steady state when compared with the initial thermal state, but it relaxes to the steady state faster. Thus, the Mpemba initial state cools the qubit faster than the usual initial thermal state. In addition to this, we also investigate the effect of the system-bath and qubit-qutrit couplings on the Mpemba effect.

The remaining part of the paper is organized as follows. In

Sec. II, we provide a brief overview of the qubit-qutrit model of the self-contained refrigerator and the quantum Mpemba effect. In Sec. III, we study the dynamics of the refrigerator, more specifically we reduce the Liouvillian that generates the dynamics of the individual elements of the system's density matrix into block diagonal form. This greatly simplifies computation of the dynamics of the system. From this block diagonal form, we solve for the steady state of the dynamics and numerically study the cooling ability of the refrigerator across a wide parameter regime. In Sec. IV, we compute the eigenvalues and the corresponding eigenvectors of the Liouvillian. The eigenvalue with largest negative real part determines the time-scale to reach the steady state. We demonstrate the Mpemba effect for the system by constructing a state where this eigenvalue is suppressed and thus it reaches to the steady state faster, demonstrating accelerated cooling. Furthermore, we also study the effect of qubit-qutrit and system-bath couplings on the Mpemba effect. Finally, we conclude in Sec. V.

II. PRELIMINARIES

The smallest self-contained refrigerator consists of a qutrit and qubit system which are coupled to three heat baths. In this system, the qutrit acts as the refrigerator and the qubit is to be cooled. The qubit is initially at equilibrium with the bath to which it is coupled. When the coupling between the qubit and qutrit is switched on, the system evolves to specific steady state, where the qubit has a lower temperature than it initially had. In this work, we accelerate this cooling using the Mpemba effect. In this section, we introduce the qubit-qutrit refrigerator model and the quantum Mpemba effect.

A. The quantum refrigerator model

The smallest self-contained model of refrigerator introduced in Ref. [35], consists of a qutrit acting as a refrigerator and a qubit to be cooled. The qubit A and qutrit B are governed by the Hamiltonians $\tilde{H}_A = JE_0|1\rangle_A\langle 1|$ and $\tilde{H}_B = J(E_1|1\rangle_B\langle 1| + E_2|2\rangle_B\langle 2|)$ respectively. For the working of the refrigerator a self-contained condition, $E_2 = E_0 + E_1$ is imposed on the system. Due to this, there is a degeneracy between the states $|02\rangle_{AB}$ and $|11\rangle_{AB}$. For the refrigerator to work, the probability of $|1\rangle_A$ is to be decreased and the probability of $|0\rangle_A$ is to be increased. This can be done, by coupling the transition $|0\rangle_B \leftrightarrow |1\rangle_B$ to a hot bath at temperature T_h, while the transition $|0\rangle_B \leftrightarrow |2\rangle_B$ is coupled to a cooler work bath at temperature T_w. The qutrit when at equilibrium with the two baths, has probabilities p_1^B and p_2^B of the two levels $|1\rangle_B$ and $|2\rangle_B$ respectively. In order to allow transitions of the kind $|02\rangle_{AB} \leftrightarrow |11\rangle_{AB}$, it is imperative to introduce an interaction $\tilde{H}_{\text{int}} = Jg(|02\rangle_{AB}\langle 11| + |11\rangle_{AB}\langle 02|)$. For small values of g, the probabilities of $|11\rangle_{AB}$ and $|02\rangle_{AB}$ are very close to each other, i.e., $p_{11}^{AB} \approx p_{02}^{AB}$. Since, $p_1^B > p_2^B$, in order to maintain the condition $p_{11}^{AB} \approx p_{02}^{AB}$, ground-state probability of qubit increases. For judicious choice of the bath temperatures, the probabilities of the two levels of the qubit can be tuned, such that the steady-state temperature is lower than the initial temperature of the qubit. This refrigerator system is presented using a schematic diagram in Fig. 1(a).

The total Hamiltonian $\tilde{H}_{AB}$ acting on the whole system is, $\tilde{H} = \tilde{H}_A + \tilde{H}_B + \tilde{H}_{\text{int}}$ Here, E_0, E_1, E_2 and g are dimensionless quantities, such that J has the necessary dimension of energy. We can write the rescaled Hamiltonian,

$$H = H_A + H_B + H_{\text{int}}, \tag{1}$$

with $H_i = \tilde{H}_i/J$, where $i = \{A, B, \text{int}\}$. Due to the degeneracy between the states $|02\rangle_{AB}$ and $|11\rangle_{AB}$ and very small value of g, we have $p_{11}^{AB} \approx p_{02}^{AB}$ at steady state. This leads to the qubit attaining a local equilibrium state with temperature T_v, such that $T_v = (E_2 - E_1)/(\frac{E_2}{T_w} - \frac{E_1}{T_h})$. The qubit attains the temperature T_v at steady state. If the qubit is also coupled to a bath at temperature T_c, then it attains a steady-state temperature in between T_c and T_v. If the steady-state temperature is lower than the initial temperature of the qubit, then qubit is said to be cooled and the qutrit is working as a refrigerator. In addition to cooling qubits, the ability of self-contained refrigerators to cool higher dimensional systems has been investigated [59–62]. The discussed qutrit-qubit system has also been used for other quantum technologies like quantum transistors [63].

As discussed earlier, the qutrit is coupled to two baths, while the qubit is coupled to one bath. The bath Hamiltonian is given by $H_\mu = \sum_k \omega_{\mu k} b_{\mu k}^\dagger b_{\mu k}$, where $\mu = \{c, h, w\}$ corresponds to the three baths c, h and w with temperatures T_c, T_h and T_w respectively. The qubit-bath and qutrit-bath interactions are given by,

$$\begin{aligned} H_{SB} = &\sum_k g_{ck}(b_{ck}^\dagger|0\rangle_A\langle 1| + b_{ck}|1\rangle_A\langle 0|) \\ &+ \sum_k g_{hk}(b_{hk}^\dagger|0\rangle_B\langle 1| + b_{hk}|1\rangle_B\langle 0|) \\ &+ \sum_k g_{wk}(b_{wk}^\dagger|0\rangle_B\langle 2| + b_{wk}|2\rangle_B\langle 0|) \end{aligned} \tag{2}$$

The total Hamiltonian of the system and bath is $H_T = \tilde{H} + \sum_{\mu=\{c,h,w\}} H_\mu + H_{SB}$. The dynamics of the refrigerator system is studied by employing the Born-Markov approximation. The density matrix ρ of the total system AB follows the Gorini-Kossakoswski-Sudarshan-Lindblad (GKSL) [64–66] master equation, $\frac{d\rho(t)}{d\tilde{t}} = -\frac{i}{\hbar}[\tilde{H}, \rho(t)] + \sum_\mu \tilde{D}_\mu[\rho(t)]$ with $\tilde{D}_\mu[\cdot] = \sum_\omega \tilde{\gamma}_\mu(\omega)(A_{\mu,\omega} \cdot A_{\mu,\omega}^\dagger - \frac{1}{2}\{A_{\mu,\omega}^\dagger A_{\mu,\omega}, \cdot\})$. Let us rescale to dimensionless quantities of $\gamma_\mu(\omega) = \frac{\hbar}{J}\tilde{\gamma}_\mu(\omega)$ and $t = \frac{J}{\hbar}\tilde{t}$. Thus, the final form of the GKSL equation is as follows,

$$\frac{d\rho(t)}{dt} = -i[H, \rho(t)] + \sum_\mu D_\mu[\rho(t)] \tag{3}$$

with $D_\mu[\rho] = \sum_\omega \gamma_\mu(\omega)(A_{\mu,\omega}\rho A_{\mu,\omega}^\dagger - \frac{1}{2}\{A_{\mu,\omega}^\dagger A_{\mu,\omega}, \rho\})$.

The decay rates are given by,

$$\gamma_\mu(\omega) = \begin{cases} J_\mu(\omega)\langle n_{\beta_\mu}(\omega)\rangle, & \text{if } \omega > 0, \\ J_\mu(\omega)\left[\langle n_{\beta_\mu}(\omega)\rangle + 1\right], & \text{if } \omega < 0. \end{cases} \tag{4}$$

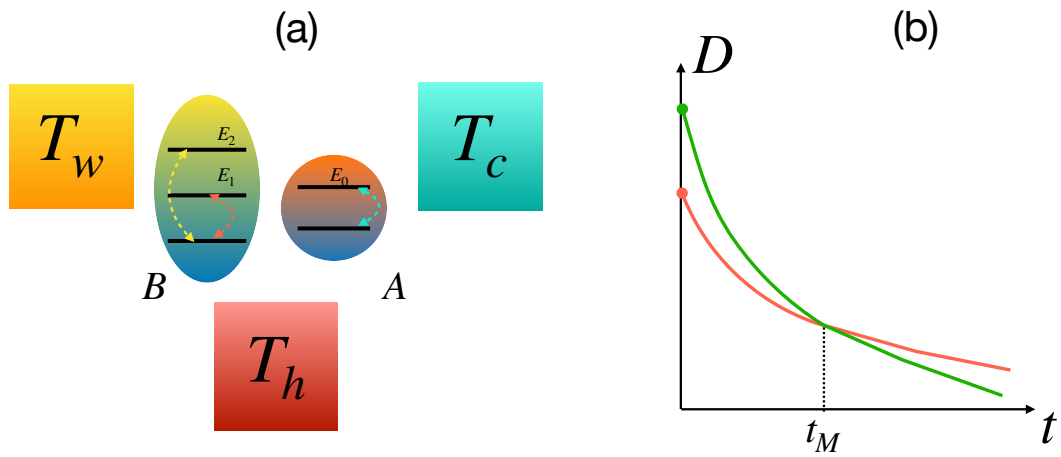

FIG. 1. ***Schematic diagram of self-contained refrigerator and Mpemba effect.*** (a) We present a schematic diagram of the qubit-qutrit self-contained refrigerator coupled to three baths. (b) We present a schematic diagram illustrating the quantum Mpemba effect. In the Mpemba effect some distance-like quantity D of the state from the steady state is observed. Two initial states are considered, with the initial state that is farther away from the equilibrium state is denoted with green, while the initial nearer is denoted with orange. In the Mpemba effect, the state initially farther away reaches equilibrium faster than the one initially nearer. The time at which both the trajectories intersect is called the Mpemba time and is represented with t_M.

Here, we consider Ohmic baths with $J_\mu(\omega) = \kappa_\mu|\omega|\exp(-|\omega|/\Omega_c)$. The average photon number is given by $\langle n_{\beta_\mu}(\omega)\rangle = \frac{1}{e^{\beta_\mu\omega}-1}$, for a bath with temperature $T_\mu = 1/\beta_\mu$. The Lindblad operators $A_{\mu,\omega}$ are presented in the Appendix A.

B. The Mpemba effect

In open quantum systems, the quantum Mpemba effect refers to the phenomenon where a system approaches its steady state faster when initialized in a state that is farther from the steady state than one that is closer to it. Let us consider a Markovian dynamics given by the dynamical equation,

$$\frac{d\rho(t)}{dt} = \mathcal{L}\rho(t). \tag{5}$$

Here, $\rho(t)$ is the density matrix describing the state of the system and $\mathcal{L}$ is the Liouvillian superoperator that generates the evolution the open quantum system. The solution to Eq. (5) is given by,

$$\rho(t) = e^{\mathcal{L}t}\rho(0) = \sum_{i=1}^{d^2} \mathrm{Tr}(l_i\rho(0))r_i e^{\lambda_i t}. \tag{6}$$

Here, $\rho(0)$ is the initial state of the system, $\{\lambda_i\}$ are the complex eigenvalues of $\mathcal{L}$, and $\{l_i\}$ and $\{r_i\}$ are its left and right eigenstates respectively, with $\mathrm{Tr}(l_i r_j) = \delta_{ij}$. For a d-dimensional system, there are d^2 eigenvalues and eigenstates. When considering the Markovian assumption, $\mathcal{L}$ and consequently $\{l_i\}$, $\{r_i\}$ and $\{\lambda_i\}$ all are time-independent. The eigenvalues are usually complex numbers with negative real numbers, except for the steady state. The steady state has eigenvalue $\lambda_1 = 0$ and the corresponding right eigenstate $r_1 = \rho_{ss}$. Moreover, the left eigenstate corresponding to the steady state is $l_1 = \mathbb{I}$, the identity operator. Thus, $\mathrm{Tr}(l_1\rho(0)) = 1$. We can rewrite Eq. (6) as,

$$\rho(t) = \rho_{ss} + \sum_{i=2}^{d^2} \mathrm{Tr}(l_i\rho(0))r_i.$$

In the long time limit, $\lim_{t\to\infty}\rho(t) = \rho_{ss}$, i.e., the system reaches the steady state. The other modes have eigenvalues with real part that is negative, which leads to their amplitudes exponentially decaying with $\lim_{t\to\infty} e^{\lambda_i t} \to 0$ for $\mathrm{Re}[\lambda_i] < 0$.

It is customary to arrange the λ_i-s in descending order of their real part, such that $0 = \mathrm{Re}[\lambda_1] > \mathrm{Re}[\lambda_2] \geq .... \geq \mathrm{Re}[\lambda_{d^2}]$. The eigenvalue λ_2 has the smallest real value in magnitude, among all the non-zero eigenvalues. This is the slowest decaying mode and determines the rate at which the system reaches the steady state. More concretely, we have $|\rho(t)-\rho_{ss}| \propto \exp(\mathrm{Re}[\lambda_2]t) = \exp(-t/\tau_2)$, with τ_2 determining the decay time-scale. Now if we consider another initial state say $\rho_M(0) = U\rho(0)U^\dagger$, such that $\mathrm{Tr}(l_2\rho_M(0)) = 0$. The evolution of this state is given by $\rho_M(t) = e^{\mathcal{L}t}\rho_M(0)$. Since, the amplitude of r_2 is completely suppressed, in this case we have $|\rho_M(t) - \rho_{ss}| \propto \exp(\mathrm{Re}[\lambda_3]t) = \exp(-t/\tau_3)$, with τ_3 determining the decay time-scale. As $|\mathrm{Re}[\lambda_2]| < |\mathrm{Re}[\lambda_3]|$, we have $\tau_2 > \tau_3$, i.e., the condition $\mathrm{Tr}(l_2\rho_M(0)) = 0$ makes the initial state $\rho_M(0)$ reach the steady state faster than the initial state $\rho(0)$. In addition to this, we consider another condition that the initial state $\rho_M(0)$ is farther away from ρ_{ss} when being compared with $\rho(0)$, i.e., we have $|\rho_M(0)-\rho_{ss}| > |\rho(0)-\rho_{ss}|$. The combination of the two conditions constitutes the quantum Mpemba effect. Throughout this paper, we call the initial state $\rho_M(0)$, the Mpemba state. The Mpemba effect is schematically presented in Fig. 1(b). We seen that there exists a specific time t_M called the Mpemba time, which marks the crossing of the two trajectories. Before the Mpemba time, the distance $|\rho_M(t) - \rho_{ss}| > |\rho(t) - \rho_{ss}|$, while post Mpemba time the inequality flips. The quantum Mpemba effect has

been observed in various quantum devices including quantum batteries [67], heat engines [68] and superconducting quantum computer [69]. Here we investigate the Mpemba effect in the self-contained quantum refrigerator.

III. DYNAMICS OF SELF-CONTAINED REFRIGERATOR

In this section, we set up the dynamical equation of the elements of the density matrix of the qutrit-qubit model of the self-contained refrigerator. We observe that the dynamics is simplified due to the block diagonal form of the Liouvillian. Moreover, we find the steady state of the dynamics and investigate the cooling capability of the refrigerator for a significant region of the parameter space.

A. Dynamical equations of self-contained refrigerator

The dynamics of the qutrit-qubit refrigerator system is governed by Eq. (3), where the Lindblad operators are presented in Eq. (A4) of the Appendix A. We can write the state of the joint-system as $\rho^{AB} = \sum_{i,j=1}^{6} \rho_{ij}|i\rangle\langle j|$, where $\{|i\rangle\}$ are the energy eigenstates as presented in Eq. (A1). Throughout this subsection, we consider the state to be written in the energy eigenbasis.

We investigate the action of the Liouvillian $\mathcal{L}[\cdot] = -i[H,\cdot] + \sum_\mu D_\mu[\cdot]$ on the state ρ^{AB}. We isolate the dynamical equation of each element ρ_{ij} of the density matrix by vectorizing the density-matrix [70], and obtaining the corresponding matrix form of the Liouvillian. Thus, we have thirty-six coupled equations of the form $d\rho_{ij}/dt = [\mathcal{L}\rho]_{ij}$, where ρ_{ij} are the elements of the matrix, when written in the energy eigenbasis. Depending on the form of $\mathcal{L}$, the dynamical equation of each element is determined. In the case of qutrit-qubit refrigerator system, the dynamical equation of the diagonal elements ρ_{ii} decouples with the off-diagonal terms and only couples among themselves. Thus, the diagonal elements evolve independently of the off-diagonal elements. This makes the matrix $\mathcal{L}[\rho]$, block diagonal, with one of the block being 6×6 for the diagonal elements given by Λ^{diag}. The diagonal elements evolve following, $d\rho_{ii}/dt = \sum_{j=1}^{6} \Lambda^{\text{diag}}_{ij}\rho_{jj}$, with Λ^{diag} being of the form,

$$\Lambda^{\text{diag}} = \frac{1}{2}\begin{bmatrix} -D_1 & 2\gamma_h(-\omega_{h,2}) & \gamma_w(-\omega_{w,1}) & 2\gamma_c(-\omega_{c,1}) & \gamma_w(-\omega_{w,2}) & 0 \\ 2\gamma_h(\omega_{h,2}) & -D_2 & \gamma_c(-\omega_{c,2}) & 0 & \gamma_c(-\omega_{c,3}) & 0 \\ \gamma_w(\omega_{w,1}) & \gamma_c(\omega_{c,2}) & -D_3 & \gamma_h(\omega_{h,1}) & 0 & \gamma_c(-\omega_{c,3}) \\ 2\gamma_c(\omega_{c,1}) & 0 & \gamma_h(-\omega_{h,1}) & -D_4 & \gamma_h(\omega_{h,3}) & 2\gamma_w(-\omega_{w,3}) \\ \gamma_w(\omega_{w,2}) & \gamma_c(\omega_{c,3}) & 0 & \gamma_h(\omega_{h,3}) & -D_5 & \gamma_c(-\omega_{c,2}) \\ 0 & 0 & \gamma_c(\omega_{c,3}) & 2\gamma_w(\omega_{w,3}) & \gamma_c(\omega_{c,2}) & -D_6 \end{bmatrix}, \tag{7}$$

where D_i-s (with $i = 1, 2, .., 6$) are presented in Eq. (B5). The decay rates are defined in Eq. (4), with the transition energies, represented by $\omega_{c,j}$, $\omega_{h,j}$ and $\omega_{w,j}$ (with $j \in \{1, 2, 3\}$) defined in Eq. (A3). On the other hand the off-diagonal terms have a much simpler dynamics. We find that certain off-diagonal terms couple with one other off-diagonal term and evolve as a pair. There are four such pairs – $\{\rho_{52}, \rho_{63}\}$, $\{\rho_{36}, \rho_{25}\}$, $\{\rho_{65}, \rho_{32}\}$ and $\{\rho_{56}, \rho_{23}\}$. The dynamical equation of these four pairs of elements each form a 2×2 matrix. The general form of these four pairs of equation is

$$\begin{aligned} \frac{d}{dt}\begin{pmatrix}\rho_{ij}\\ \rho_{kl}\end{pmatrix} &= \Lambda_{ij,kl}\begin{pmatrix}\rho_{ij}\\ \rho_{kl}\end{pmatrix}, \quad \text{where} \\ \Lambda_{63,52} &= \begin{pmatrix}\lambda_{63} & \gamma_c(\omega_{c,2})\\ \gamma_c(-\omega_{c,2}) & \lambda_{52}\end{pmatrix}, \\ \Lambda_{36,25} &= \begin{pmatrix}\lambda_{36} & \gamma_c(\omega_{c,2})\\ \gamma_c(-\omega_{c,2}) & \lambda_{25}\end{pmatrix}, \\ \Lambda_{65,32} &= \begin{pmatrix}\lambda_{65} & -\gamma_c(\omega_{c,3})\\ -\gamma_c(-\omega_{c,3}) & \lambda_{32}\end{pmatrix} \quad \text{and} \\ \Lambda_{56,23} &= \begin{pmatrix}\lambda_{56} & -\gamma_c(\omega_{c,3})\\ -\gamma_c(-\omega_{c,3}) & \lambda_{23}\end{pmatrix}. \end{aligned} \tag{8}$$

It can be seen that the matrices $\Lambda_{ij,kl}$ have the decay rates of the cold bath c in its off-diagonal. So, the dynamics of these elements become completely independent when the cold bath c is absent and we have $\gamma_c(\omega) = 0$ for all ω. The remaining twenty-two off-diagonal terms do not couple with each other. The dynamical equations of these elements are of the from, $d\rho_{ij}/dt = \lambda_{ij}\rho_{ij}$ with the solution $\rho_{ij}(t) = \rho_{ij}(0)e^{\lambda_{ij}t}$, where λ_{ij} are complex numbers with negative real parts. The explicit forms of all thirty λ_{ij} is given by,

$$\lambda_{ij} = -i\mathcal{E}_{ij} - \frac{1}{4}G_{ij}. \tag{9}$$

Here, the first term $\mathcal{E}_{ij} = \mathcal{E}_i - \mathcal{E}_j$ is due to the unitary dynamics, whereas the second term $G_{ij} = D_i + D_j$ is due to the coupling with the baths. The eigenvalues of the system $\mathcal{E}_i$ are given by Eq. (A2) and the explicit expressions of D_i are given by Eq. (B5). The real part of all off-diagonal elements, $\text{Re}[\lambda_{ij}] = -G_{ij}/4$, are negative. This ensures that the off-diagonal terms decay with time and vanish at the steady state, decohering the state. The block diagonal form of $\mathcal{L}$ is illustrated with the help of a schematic in Fig. 2(a).

Thus, the dynamics of the thirty-six elements, reduces to solving the dynamics of one six-dimensional dynamical system, four two-dimensional system and twenty-two one dimensional systems. This is much more tractable problem than a fully thirty-six-dimensional system. Although still solving the

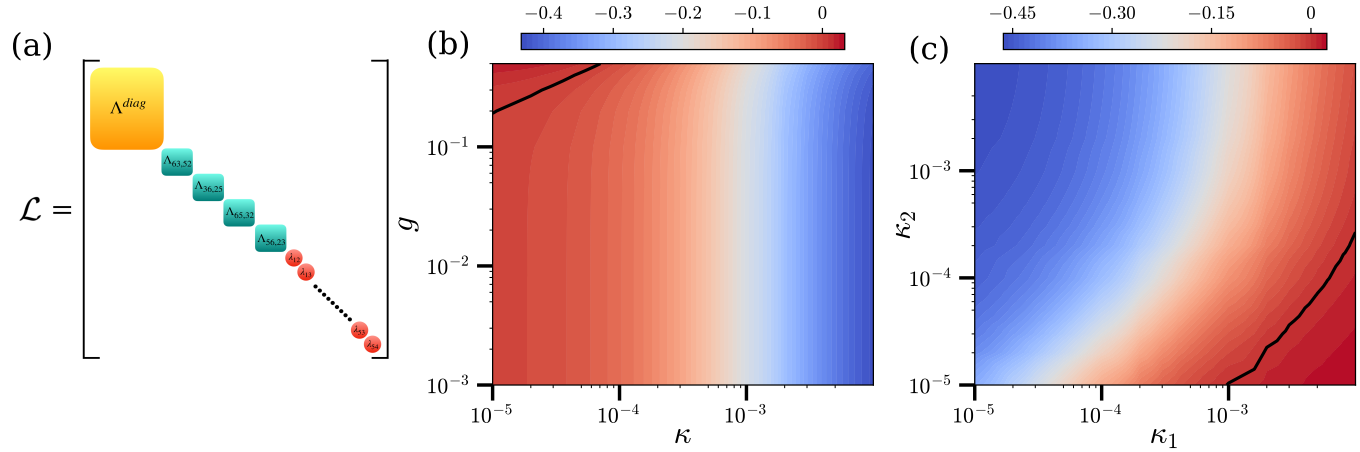

FIG. 2. ***Generator of dynamics and steady state of self-contained quantum refrigerator.*** (a) We present a schematic showing the block-diagonal form of the Liouvillian of the self-contained qubit-qutrit refrigerator. The largest block Λ^{diag} in yellow, corresponds to the dynamics of the diagonal elements of the density matrix in the energy eigenbasis and is given by Eq. (7). The smaller four blocks in green, are of dimension 2×2 each and are given by Eq. (8). The other elements do not couple to any other element are their eigenvalues λ_{ij} is given in Eq (9). (b) We present the change in the quantity $\Delta T = T_s - T_c^0$ with the variation in qubit-qutrit coupling g and coupling between system and h and w bath with $\kappa_h = \kappa_w = \kappa$ and $\kappa_c = 10^{-3}$. Here, T_s is the temperature of the qubit at the steady state whereas T_c^0 is the initial temperature of the qubit. Thus, ΔT measures the cooling capacity of the quantum refrigerator. (c) We present the variation of ΔT with the variation of $\kappa_c = \kappa_1$ and $\kappa_h = \kappa_2$ with $\kappa_w = 10^{-3}$ and $g = 0.5$. In both the cases, $E_0 = 0.7$, $E_1 = 1.0$ with $T_h = 3.0$ and $T_c = T_w = 1.0$, consequently $T_c^0 = 1$. The solid-black line denotes $\Delta T = 0$, beyond which the system no longer provides steady-state cooling.

six-dimensional dynamical system analytically is very challenging. Therefore, we restore to numerical methods for solving it. We construct the left and right eigenvectors of the whole dynamics by solving for the individual block and use Eq. (6) to given a solution for the total state $\rho^{AB}(t)$ for any time t. The blocks given by Eq. (7), Eq. (8) and Eq. (9) completely determine the dynamics of the qubit-qutrit model coupled to three heat baths. In the absence of the cold bath c, we can just set the decay rates corresponding to the c-bath to zero.

B. Steady state of self-contained refrigerator

The qutrit-qubit refrigerator system has a unique steady state, which it attains after a long time. In this subsection, we find the steady state of the system which corresponds to the right-eigenvector of the Liouvillian $\mathcal{L}$ with zero-eigenvalue. We observe that the block-diagonal Λ^{diag} corresponding to the evolution of diagonal entries $(\rho_{ii}(t))$ of the density-matrix of the system has a zero-eigenvalue. Thus the steady state τ is diagonal in the energy eigenbasis, i.e., $\tau = \sum_{i=1}^{6} \tau_i |i\rangle\langle i|$. We need to solve the linear equation,

$$\Lambda^{\text{diag}} \tau = 0, \tag{10}$$

with the additional constraint of unit trace, i.e., $\sum_{i=1}^{6} \tau_i = 1$. Although Eq. (10) is analytically solvable, the complete expression of τ is tedious and difficult to present here. Therefore, we resort to numerically solve the set of simultaneous linear equation obtained from Eq. (10) while respecting the normalization condition on trace. For the qubit-qutrit system to act as a refrigerator, it is essential that the steady-state temperature T_s of the qubit is lower than the initial temperature of the qubit T_c^0. We define the temperature of the qubit as,

$$T(t) = \frac{E_0}{k_B \ln\left[p_0^A(t)/p_1^A(t)\right]}, \tag{11}$$

where k_B is the Boltzmann constant, $p_0^A(t)$ and $p_1^A(t)$ are the probabilities of the ground state and excited state at time t. Throughout this paper, we have set $k_B = 1$. Thus, the steady-state temperature and initial temperature are given by, $T_s := T(t \to \infty)$ and $T_c^0 := T(0)$ respectively. For states which are not diagonal in the energy basis, usually the definition of temperature is considered to be the temperature of the thermal state closest to the state under consideration based on the trace distance measure [62]. For qubits, this criteria leads to the definition in Eq. (11). Thus, at least for qubits, there is no ambiguity regarding the two definitions.

In our analysis, we consider the qubit-qutrit system with $E_0 = 0.7$ and $E_1 = 1.0$. Moreover, we set the temperature of the c, h and w baths to be $T_c = 1$, $T_h = 3$ and $T_w = 1$, respectively. The initial state of the qubit is taken to be the equilibrium Gibbs state at temperature T_c, i.e., $\rho_A(t = 0) = e^{-H_A/T_c}/\mathcal{Z}_{A,c}$, with initial temperature being $T_c^0 = T_c$. In the case, where the c-bath coupled with qubit A is absent and the qubit-qutrit coupling g is very small, $T_s \approx T_v = (E_2 - E_1)/(\frac{E_2}{T_w} - \frac{E_1}{T_h}) \approx 0.5122$. The cooling ability of the refrigerator on the qubit is given by $\Delta T := T_s - T_c^0 \approx -0.4878$, with the initial qubit state considered to be a Gibbs state with temperature $T_c^0 = 1$. For larger values of g and the presence of the c-bath, it is harder to estimate the steady-sate temperature of the qubit and requires solving for τ from Eq. (10). We specifically analyze the effect of the couplings between the system and baths κ_c, κ_w and κ_h as well as the qubit-qutrit coupling g on steady-state temperature. We present the vari-

ation of $\Delta T = T_s - T_c^0$ of the qubit with system parameters in Fig. 2(b) and (c). In Fig. 2(b), setting $\kappa_c = 10^{-3}$, we vary $\kappa_h = \kappa_w = \kappa$ and g and observe that the qubit undergoes cooling except for the region of large values of g and small values of κ. The contour with $\Delta T = 0$ is shown with a black solid line. The steady-state temperature T_s is independent of g when g is small, while for larger values of g the steady-state temperature increases with increase in g. On the other hand, cooling improves for larger values of κ. In Fig. 2(c) we set $g = 0.5$ and $\kappa_w = 10^{-3}$, while we vary $\kappa_c = \kappa_1$ and $\kappa_h = \kappa_2$. As in the previous case, the contour with $\Delta T = 0$ is presented in solid black line. The cooling is improved for smaller values of κ_1 and larger value of κ_2. For the parameter regime where $\Delta T \geq 0$, the system no longer works as a refrigerator. This is consistent with the cases with smaller g, where the steady-state temperature decrease as the coupling with cold bath decreases and reaches its minimum the absence of the c-bath.

IV. MPEMBA EFFECT IN QUANTUM REFRIGERATOR

In the previous section, we discussed about the dynamics generated by the Liouvillian operator and the corresponding steady state of the qubit-qutrit model of the self-contained refrigerator. In this section, we consider the qubit-qutrit system being initialized in equilibrium with their respective baths, and investigate if it is possible to accelerate the cooling of the qubit with the help of Mpemba effect. To observe the Mpemba effect, we consider both local and global unitary operation on the initial state.

The quantum refrigerator consisting of the qubit A and qutrit B is governed by the free Hamiltonian of $H_{\text{free}} = H_A + H_B$ and is coupled with three baths as discussed in Sec. II A. Initially, the qubit-qutrit coupling is switched off. The initial state of the system is,

$$\rho_{\text{th}}^{AB}(0) = \gamma_A^{\beta_c} \otimes \gamma_B^{\beta_h,\beta_w}, \tag{12}$$

where $\gamma_A^{\beta_c} := (|0\rangle_A\langle 0| + e^{-\beta_c E_0}|1\rangle_A\langle 1|)/(1 + e^{-\beta_c E_0})$ and $\gamma_B^{\beta_h,\beta_w} := (|0\rangle_B\langle 0| + e^{-\beta_h E_1}|1\rangle_B\langle 1| + e^{-\beta_w E_2}|2\rangle_B\langle 2|)/(1 + e^{-\beta_h E_1} + e^{-\beta_w E_2})$ with $\beta_\mu = 1/(k_B T_\mu)$. Now at $t = 0$, the interaction $H_{\text{int}} = g|02\rangle_{AB}\langle 11| + \text{h.c.}$, is switched on and the system evolves according to Eq. (5) with the total Hamiltonian being $H = H_A + H_B + H_{\text{int}}$. This leads to the system relaxing towards a specific steady state given by τ from Eq. (10).

On decomposing the Liouvillian $\mathcal{L}$, we observe that the initial state $\rho_{\text{th}}^{AB}(0)$ have contributions from the slowest eigenstate, i.e., $\text{Tr}(l_2\rho_{\text{th}}^{AB}(0)) \neq 0$. This means that the evolution to steady state when starting with $\rho_{\text{th}}^{AB}(0)$ as the initial state is dominated by $\exp[\lambda_2 t]$ term. We try to find if it is possible to start with an initial state that has no or negligible contribution from the eigenstate corresponding to λ_2 and reaches the steady state faster than $\rho_{\text{th}}^{AB}(0)$, leading to accelerated cooling. Moreover, for Mpemba effect another condition required is that the initial state that reaches steady state quicker also needs to be initially farther away from the steady state. For this we consider the trace-distance between the evolving state and steady state. The trace-distance measure is defined as,

$$D(\sigma, \eta) = \frac{1}{2}\|\sigma - \eta\|_1, \tag{13}$$

where $\|A\|_1 = \text{Tr}(\sqrt{AA^\dagger})$.

We demonstrate the Mpemba effect in the quantum refrigerator system by comparing the dynamics of $\rho_{\text{th}}^{AB}(0)$ and another state $\rho_{\text{M}}^{AB}(0) = U\rho_{\text{th}}^{AB}(0)U^\dagger$. We call this state the Mpemba state. To ensure this, we demand $D(\rho_{\text{th}}^{AB}(0), \tau) < D(\rho_{\text{M}}^{AB}(0), \tau)$ and $\rho_{\text{M}}^{AB}(0)$ reaches steady state faster than $\rho_{\text{th}}^{AB}(0)$.

For this, we consider unitary operations that are both local and global on the qubit-qutrit system. This leads to initial states of four kinds,

$$\begin{aligned}
\rho_{1,\text{g}}^{AB}(0) &:= U_{1,\text{g}}\rho_{\text{th}}^{AB}(0)U_{1,\text{g}}^\dagger \\
\rho_{2,\text{l}}^{AB}(0) &:= U_{2,\text{l}}\rho_{\text{th}}^{AB}(0)U_{2,\text{l}}^\dagger \\
\rho_{3,\text{l}}^{AB}(0) &:= U_{3,\text{l}}\rho_{\text{th}}^{AB}(0)U_{3,\text{l}}^\dagger \\
\rho_{4,\text{l}}^{AB}(0) &:= U_{4,\text{l}}\rho_{\text{th}}^{AB}(0)U_{4,\text{l}}^\dagger.
\end{aligned} \tag{14}$$

Here, $U_{1,\text{g}}$ is a global unitary acting on the joint qubit-qutrit system, $U_{2,\text{l}}$, $U_{3,\text{l}}$ and $U_{4,\text{l}}$ are local unitaries of the form $V_A \otimes V_B$, $V_A \otimes \mathbb{I}_B$ and $\mathbb{I}_A \otimes V_B$ respectively, with $\mathbb{I}_{A(B)}$ being the identity operator on $A(B)$ and V_A and V_B being some unitary operation on A and B respectively. We numerically find such unitary by using NLOPT [71]. We set the objective to maximize the difference between the initial distances between $D(\rho_{\text{M}}^{AB}(0), \tau) - D(\rho_{\text{th}}^{AB}(0), \tau)$, with the equality constraint that $\text{Tr}(l_2\rho_M^{AB}(0)) = 0$ for $\rho_M^{AB}(0)$ being the four states defined in Eq. (14). We find the optimized unitaries for the global and local cases and their respective initial states.

In Fig. 3(a) and (b) we consider different initial states and demonstrate Mpemba effect in the refrigerator system. In Fig. 3(a), we present the two states of the form $\rho_{\text{th}}^{AB}(0)$ and $\rho_{1,\text{g}}^{AB}(0)$ in solid-blue and dashed orange line respectively. We present the trace distance of states from the steady state τ and observe that the state $\rho_{1,\text{g}}^{AB}(0)$, despite being initially farther away from the steady state, reaches steady state faster than $\rho_{\text{th}}^{AB}(0)$. This is the quantum Mpemba effect. In Fig. 3(b), we present the trace distance from steady state for the initial states $\rho_{2,\text{l}}^{AB}(0)$, $\rho_{3,\text{l}}^{AB}(0)$ and $\rho_{4,\text{l}}^{AB}(0)$ in solid-blue, dashed-orange and dash-dotted-green lines respectively. We observe that only $\rho_{2,\text{l}}^{AB}(0)$ shows the Mpemba effect when compared with the initial state $\rho_{\text{th}}^{AB}(0)$. It was possible to suppress the slowest decaying mode with local unitary of the form of $U_{2,\text{l}}$ but not possible with local unitaries like $U_{3,\text{l}}$ and $U_{4,\text{l}}$ On further investigation we realize that $\rho_{1,\text{g}}^{AB}(0)$ reaches steady state faster than $\rho_{2,\text{l}}^{AB}(0)$ in all parameter regime we investigated.

Furthermore, we present the Mpemba effect for the case with no c-bath in Fig. 3(c). Since the evolution now differs, the four initial states given in Eq. (14) also differ from those in the previous scenario. To distinguish them, we denote the initial states in the absence of the c-bath with an additional tilde. In Fig. 3(c), the state $\rho_{\text{th}}^{AB}(0)$ is presented in solid-blue line while the state $\tilde{\rho}_{1,\text{g}}^{AB}(0)$ in dashed-orange line. The state $\tilde{\rho}_{1,\text{g}}^{AB}(0)$ reaches the steady state faster than the thermal state and was initially father away from as shown in the inset. This demonstrates the Mpemba effect.

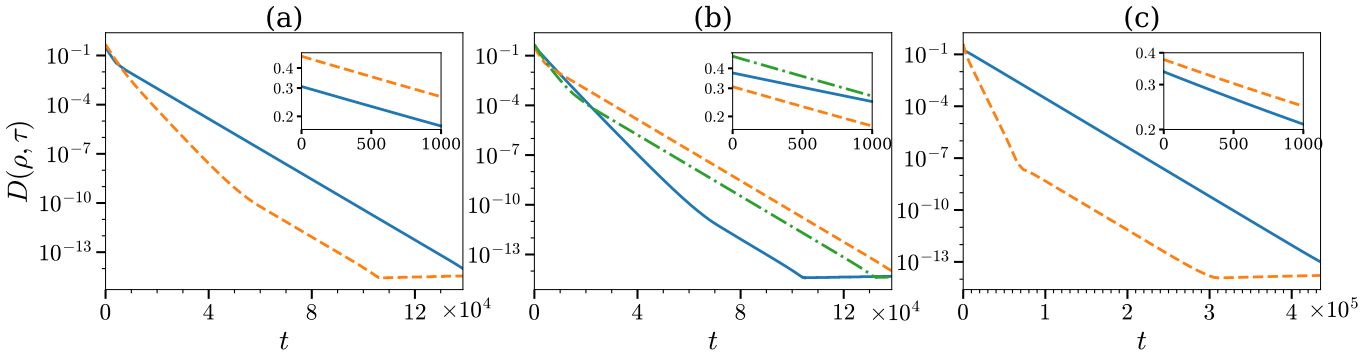

FIG. 3. ***Mpemba effect in self-contained quantum refrigerator.*** (a) We present the trace distance $D(\rho_{\rm th}^{AB}(t),\tau)$ in solid-blue and $D(\rho_{1,\rm g}^{AB}(t),\tau)$ in dashed-orange line. In the inset we show that initially, $D(\rho_{\rm th}^{AB}(0),\tau) < D(\rho_{1,\rm g}^{AB}(0),\tau)$, despite this $\rho_{1,\rm g}^{AB}(t)$ reaches steady state faster than $\rho_{\rm th}^{AB}(0)$. (b) We present the evolution of trace distance with τ of the initial states $D(\rho_{2,\rm l}^{AB}(0),\tau)$, $D(\rho_{3,\rm l}^{AB}(0),\tau)$ and $D(\rho_{4,\rm l}^{AB}(0),\tau)$ in solid-blue, dashed-orange and dot-dashed-green lines respectively. The state $\rho_{2,\rm l}^{AB}(0)$ demonstrates the Mpemba effect, while the other two states do not show the Mpemba effect. (c) We show the Mpemba effect in the absence of cold bath. We present the the trace distance $D(\rho_{\rm th}^{AB}(t),\tilde{\tau})$ in solid-blue and $D(\tilde{\rho}_{1,\rm g}^{AB}(t),\tilde{\tau})$ in dashed-orange line in the absence of the c-bath. In the inset we show that initially $D(\rho_{\rm th}^{AB}(0),\tilde{\tau}) < D(\tilde{\rho}_{1,\rm g}^{AB}(0),\tilde{\tau})$. Here the initial state $\rho_{\rm th}^{AB}(0)$ is same as in (a), but since the dynamics is different in the absence of c-bath, we represent the steady state as $\tilde{\tau}$ and the Mpemba state obtained from global unitary as $\tilde{\rho}_{1,\rm g}^{AB}(0)$. In all three cases, $E_0 = 0.7$, $E_1 = 1.0$, $T_c = T_w = 1.0$, $T_h = 3.0$, $g = 10^{-3}$ and $\kappa_h = \kappa_w = 10^{-4}$. In (a) and (b), $\kappa_c = 10^{-4}$ while in (c) $\kappa_c = 0$.

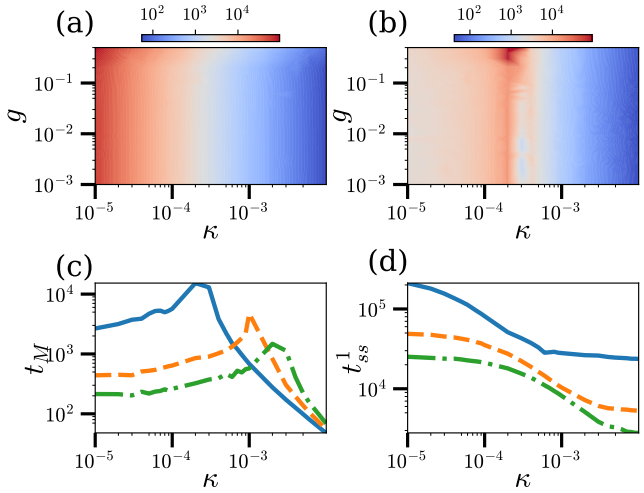

FIG. 4. ***Variation of steady-state time and Mpemba-time in quantum refrigerator.*** (a) The variation of Mpemba-time t_M, is presented with respect to the change in qubit-qutrit coupling g and the system-environment couplings $\kappa_c = \kappa_w = \kappa_h = \kappa$. (b) We present the same quantity, t_M with the change in g and $\kappa_c = \kappa$, fixing $\kappa_w = \kappa_h = 10^{-4}$. (c) Setting $g = 0.2$, we present the variation of t_M with the variation of $\kappa_c = \kappa$. (d) Keeping the parameters same as (c), we present the steady-state time t^1_{ss} of the state $\rho_{1,{\rm g}^{AB}}$. In both (c) and (d), the solid-blue line is for $\kappa_h = \kappa_w = 10^{-4}$, the dashed-orange line for $\kappa_h = \kappa_w = 5\times 10^{-4}$ and the dot-dashed-green line for $\kappa_h = \kappa_w = 10^{-3}$. The other parameters are same as those considered in Fig. 3.

Throughout Fig. 3, $E_0 = 0.7$, $E_1 = 1.0$, $T_c = T_r = 1.0$, $T_h = 3.0$ and $g = 10^{-3}$. The system-bath couplings are $\kappa_h = \kappa_w = 10^{-4}$, for all three sub-figures, with $\kappa_c = 10^{-4}$ for Fig. 3(a) and (b) while to simulate the absence of cold bath $\kappa_c = 0$ in Fig. 3(c). The cases presented in Fig. 3 is just a representative case. We do observe Mpemba effect in the quantum refrigerator for a large region of the parameter space.

In addition to this, we investigate the effect of the qubit-qutrit coupling g and system-environment coupling κ_μ on the Mpemba effect observed in the refrigerator system. In Mpemba effect, the time at which the initially distant state's trajectory crosses over that of the initially nearer state is known as Mpemba time. In our analysis, we consider the Mpemba time t_M, when the trace distance of the two states from the steady state intersect with each other. We also investigate the time it takes for the various initial states to reach the steady state. The steady-state time of the initial state $\rho_{1,\rm g}^{AB}(0)$ is given by t^1_{ss}.

In Fig. 4(a), we present the variation of Mpemba time t_M with the change in qubit-qutrit coupling g and the system-environment couplings, all of which are set equal and varied, i.e. $\kappa_c = \kappa_w = \kappa_h = \kappa$. We observe that t_M does not quite depend on g, but monotonically decreases with increase in system-environment coupling κ. In Fig. 4(b), we present the same quantity t_M, but with constant $\kappa_w = \kappa_h = 10^{-4}$ and varying $\kappa_c = \kappa$ and g. We observe that for smaller values of g, it does not influence t_M, but for larger values, t_M increases for certain values of κ_c. Moreover, the dependence of t_M on κ is no longer monotonous, rather it peaks at a certain point close to the coupling values of the other two baths. We further investigate this in Fig. 4(c) and (d), where we set $g = 0.2$ and consider the variation of t_M and t^1_{ss} with the variation of $\kappa_c = \kappa$, where the solid-blue line is for $\kappa_h = \kappa_w = 10^{-4}$, the dashed-orange line for $\kappa_h = \kappa_w = 5\times 10^{-4}$ and the dot-dashed-green line for $\kappa_h = \kappa_w = 10^{-3}$. In Fig. 4(c), we observe that the highest values of t_M are obtained for κ that are near the coupling of the other baths. In Fig. 4(d), we observe that the t^1_{ss} monotonically decreases with the increase in $\kappa_c = \kappa$. The steady-state time for the thermal initial state also show similar dependence as shown in (d). Throughout Fig. 4,

the parameters are set as, $E_0 = 0.7$, $E_1 = 1.0$, $T_h = 3.0$ and $T_w = T_c = 1.0$. Thus, the Mpemba effect can accelerate the cooling of a qubit using quantum refrigerator.

V. CONCLUSION

The quantum Mpemba effect is a curious phenomenon where a state, which can be called the Mpemba state, is initially farther away from the steady state in comparison to some other initial state, but it reaches the steady state faster than the other initial state. In open quantum systems, this can be achieved by solving the dynamics of the system, specifically by finding the eigenvalues of the Liouvillian that generates the dynamics of the system. All the eigenvalues have negative real parts, and the eigenvalue with the smallest absolute value of the real part corresponds to the slowest decaying mode and determines the time it takes to reach the steady state. The Mpemba effect is realized by suppressing the amplitude of this slowest decaying mode in the initial state of the dynamics.

In our work, we considered the qubit-qutrit self-contained quantum refrigerator and studied its dynamics. We numerically found the steady state and investigated how much cooling can be achieved for various system parameters. Subsequently, we demonstrated the Mpemba effect in this system. We found the eigenvalues and eigenvectors of the Liouvillian corresponding to the dynamics of the system. The refrigerator is usually initialized in a state where the qubit and qutrit are locally in equilibrium with their corresponding baths. To start the refrigeration dynamics, a qubit-qutrit coupling is switched on. We constructed both local and global unitary operators acting on this initial equilibrium state, so that the states obtained act as Mpemba states. These states are initially farther away from the steady state but reach the steady state faster than the initial equilibrium state. Thus, we can achieve the steady-state cooling quicker on starting with these Mpemba initial states. Furthermore, we studied the effect of change in system-bath and qubit-qutrit couplings on the Mpemba time, and on the steady state corresponding to the Mpemba initial state. Various quantum devices like heat engines, batteries, and heat transistors require the system to reach the steady state for efficient functioning. Due to weak-coupling with the environment, such systems take a long time to reach the steady state. We believe that the study makes it plausible to utilize the Mpemba effect in accelerating the dynamics of such quantum devices.

APPENDICES

A. LINDBLAD OPERATORS OF QUANTUM REFRIGERATOR

Here we present the Linblad operators of the refrigerator system coupled with three baths. The eigenstates of the Hamiltonian H of Eq. (1) are as follows,

$$|1\rangle = |00\rangle, \quad |2\rangle = |01\rangle, \quad |3\rangle = \frac{1}{\sqrt{2}}(|11\rangle - |02\rangle),$$
$$|4\rangle = |10\rangle, \quad |5\rangle = \frac{1}{\sqrt{2}}(|11\rangle + |02\rangle), \quad |6\rangle = |12\rangle. \tag{A1}$$

The corresponding eigenvalues are -

$$\mathcal{E}_1 = 0, \quad \mathcal{E}_2 = E_1, \quad \mathcal{E}_3 = E_2 - g, \quad \mathcal{E}_4 = E_0,$$
$$\mathcal{E}_5 = E_2 + g \quad \text{and} \quad \mathcal{E}_6 = E_0 + E_2 \quad \text{respectively.} \tag{A2}$$

For the system bath interactions given by Eq. (2), the GKSL equation in Eq. (3) is derived. The possible transitions energies are,

$$\omega_{c,1} = E_0, \quad \omega_{c,2} = E_0 - g, \quad \omega_{c,3} = E_0 + g,$$
$$\omega_{h,1} = E_1 + g, \quad \omega_{h,2} = E_1, \quad \omega_{h,3} = E_1 + g,$$
$$\omega_{w,1} = E_2 - g, \quad \omega_{w,2} = E_2 + g, \quad \omega_{w,3} = E_2. \tag{A3}$$

The corresponding Lindblad operators are given by,

$$\begin{aligned}
A_{c,E_1} &= |1\rangle\langle 4|,\\
A_{c,E_1-g} &= \frac{1}{\sqrt{2}}(|2\rangle\langle 3| + |5\rangle\langle 6|),\\
A_{c,E_1+g} &= \frac{1}{\sqrt{2}}(|2\rangle\langle 5| - |3\rangle\langle 6|)\\
A_{h,E_2-g} &= \frac{1}{\sqrt{2}}|4\rangle\langle 3|,\\
A_{h,E_2} &= |1\rangle\langle 2|,\\
A_{h,E_2+g} &= \frac{1}{\sqrt{2}}|4\rangle\langle 5|\\
A_{w,E_3-g} &= \frac{1}{\sqrt{2}}|1\rangle\langle 3|,\\
A_{w,E_3+g} &= -\frac{1}{\sqrt{2}}|1\rangle\langle 5|,\\
A_{w,E_3} &= |4\rangle\langle 6|.
\end{aligned} \tag{A4}$$

B. THE EXPRESSION OF D_i FROM Λ^{diag} AND λ_{ij}

Here we present the explicit expression of all D_i as they appear in the expressions of Λ^{diag} and λ_{ij} in Eq. (7) and Eq. (9) respectively.

$$\begin{aligned}
D_1 &= 2\gamma_h(\omega_{h,2}) + \gamma_w(\omega_{w,1}) + 2\gamma_c(\omega_{c,1}) + \gamma_w(\omega_{w,2}),\\
D_2 &= 2\gamma_h(-\omega_{h,2}) + \gamma_c(\omega_{c,2}) + \gamma_c(\omega_{c,3}),\\
D_3 &= \gamma_h(-\omega_{h,1}) + \gamma_w(-\omega_{w,1}) + \gamma_c(-\omega_{c,2}) + \gamma_c(\omega_{c,3}),\\
D_4 &= \gamma_h(\omega_{h,1}) + \gamma_h(\omega_{h,3}) + 2\gamma_w(\omega_{w,3}) + 2\gamma_c(-\omega_{c,1}),\\
D_5 &= \gamma_h(-\omega_{h,3}) + \gamma_w(-\omega_{w,2}) + \gamma_c(\omega_{c,2}) + \gamma_c(-\omega_{c,3}), \text{ and}\\
D_6 &= 2\gamma_w(-\omega_{w,3}) + \gamma_c(-\omega_{c,2}) + \gamma_c(-\omega_{c,3}).
\end{aligned} \tag{B5}$$

[1] F. Ares, P. Calabrese, and S. Murciano, The quantum mpemba effects, Nature Reviews Physics (2025).

[2] G. Teza, J. Bechhoefer, A. Lasanta, O. Raz, and M. Vucelja, Speedups in nonequilibrium thermal relaxation: Mpemba and related effects, arXiv:2502.01758 (2025).

[3] F. Carollo, A. Lasanta, and I. Lesanovsky, Exponentially accelerated approach to stationarity in markovian open quantum systems through the mpemba effect, Phys. Rev. Lett. **127**, 060401 (2021).

[4] S. Kochsiek, F. Carollo, and I. Lesanovsky, Accelerating the approach of dissipative quantum spin systems towards stationarity through global spin rotations, Phys. Rev. A **106**, 012207 (2022).

[5] F. Ares, S. Murciano, and P. Calabrese, Entanglement asymmetry as a probe of symmetry breaking, Nat Commun **14** (2023).

[6] C. Rylands, K. Klobas, F. Ares, P. Calabrese, S. Murciano, and B. Bertini, Microscopic origin of the quantum mpemba effect in integrable systems, Phys. Rev. Lett. **133**, 010401 (2024).

[7] S. Yamashika, F. Ares, and P. Calabrese, Entanglement asymmetry and quantum mpemba effect in two-dimensional free-fermion systems, Phys. Rev. B **110**, 085126 (2024).

[8] K. Chalas, F. Ares, C. Rylands, and P. Calabrese, Multiple crossings during dynamical symmetry restoration and implications for the quantum mpemba effect, J. Stat. Mech. **2024**, 103101 (2024).

[9] F. Ares, V. Vitale, and S. Murciano, Quantum mpemba effect in free-fermionic mixed states, Phys. Rev. B **111**, 104312 (2025).

[10] L. K. Joshi, J. Franke, A. Rath, F. Ares, S. Murciano, F. Kranzl, R. Blatt, P. Zoller, B. Vermersch, P. Calabrese, C. F. Roos, and M. K. Joshi, Observing the quantum mpemba effect in quantum simulations, Phys. Rev. Lett. **133**, 010402 (2024).

[11] A. K. Chatterjee, S. Takada, and H. Hayakawa, Quantum mpemba effect in a quantum dot with reservoirs, Phys. Rev. Lett. **131**, 080402 (2023).

[12] J. Graf, J. Splettstoesser, and J. Monsel, Role of electron–electron interaction in the mpemba effect in quantum dots, J. Phys.: Condens. Matter **37**, 195302 (2025).

[13] X. Wang and J. Wang, Mpemba effects in nonequilibrium open quantum systems, Phys. Rev. Res. **6**, 033330 (2024).

[14] K. Zatsarynna, A. Nava, R. Egger, and A. Zazunov, Green's function approach to josephson dot dynamics and application to quantum mpemba effects, Phys. Rev. B **111**, 104506 (2025).

[15] S. K. Manikandan, Equidistant quenches in few-level quantum systems, Phys. Rev. Res. **3**, 043108 (2021).

[16] F. Ivander, N. Anto-Sztrikacs, and D. Segal, Hyperacceleration of quantum thermalization dynamics by bypassing long-lived coherences: An analytical treatment, Phys. Rev. E **108**, 014130 (2023).

[17] Y.-L. Zhou, X.-D. Yu, C.-W. Wu, X.-Q. Li, J. Zhang, W. Li, and P.-X. Chen, Accelerating relaxation through liouvillian exceptional point, Phys. Rev. Res. **5**, 043036 (2023).

[18] A. K. Chatterjee, S. Takada, and H. Hayakawa, Multiple quantum mpemba effect: Exceptional points and oscillations, Phys. Rev. A **110**, 022213 (2024).

[19] F. Kheirandish, N. Cheraghpour, and A. Moradian, The mpemba effect in quantum oscillating and two-level systems, arXiv:2412.03943 (2024).

[20] A. Nava and R. Egger, Mpemba effects in open nonequilibrium quantum systems, Phys. Rev. Lett. **133**, 136302 (2024).

[21] S. Longhi, Mpemba effect and super-accelerated thermalization in the damped quantum harmonic oscillator, Quantum **9**, 1677 (2025).

[22] A. Nava and M. Fabrizio, Lindblad dissipative dynamics in the presence of phase coexistence, Phys. Rev. B **100**, 125102 (2019).

[23] R. Bao and Z. Hou, Accelerating relaxation in markovian open quantum systems through quantum reset processes, arXiv:2212.11170 (2022).

[24] S. Longhi, Bosonic mpemba effect with non-classical states of light, APL Quantum **1** (2024).

[25] P. Westhoff, S. Paeckel, and M. Moroder, Fast and direct preparation of a genuine lattice bec via the quantum mpemba effect, arXiv:2504.05549 (2025).

[26] S. Longhi, Photonic mpemba effect, Optics Letters **49**, 5188 (2024).

[27] S. Aharony Shapira, Y. Shapira, J. Markov, G. Teza, N. Akerman, O. Raz, and R. Ozeri, Inverse mpemba effect demonstrated on a single trapped ion qubit, Phys. Rev. Lett. **133**, 010403 (2024).

[28] J. Zhang, G. Xia, C.-W. Wu, T. Chen, Q. Zhang, Y. Xie, W.-B. Su, W. Wu, C.-W. Qiu, P.-X. Chen, W. Li, H. Jing, and Y.-L. Zhou, Observation of quantum strong mpemba effect, Nat Commun **16** (2025).

[29] M. Moroder, O. Culhane, K. Zawadzki, and J. Goold, Thermodynamics of the quantum mpemba effect, Phys. Rev. Lett. **133**, 140404 (2024).

[30] L. P. Bettmann and J. Goold, Information geometry approach to quantum stochastic thermodynamics, Phys. Rev. E **111**, 014133 (2025).

[31] D. J. Strachan, A. Purkayastha, and S. R. Clark, Non-markovian quantum mpemba effect, Phys. Rev. Lett. **134**, 220403 (2025).

[32] J. Furtado and A. C. Santos, Strong quantum mpemba effect with squeezed thermal reservoirs, arXiv:2411.04545 (2024).

[33] M. Zhao and Z. Hou, Noise-induced quantum mpemba effect, arXiv:2507.11915 (2025).

[34] S. Longhi, Quantum mpemba effect from initial system–reservoir entanglement, APL Quantum **2** (2025).

[35] N. Linden, S. Popescu, and P. Skrzypczyk, How small can thermal machines be? the smallest possible refrigerator, Phys. Rev. Lett. **105**, 130401 (2010).

[36] P. Skrzypczyk, N. Brunner, N. Linden, and S. Popescu, The smallest refrigerators can reach maximal efficiency, J. Phys. A: Math. Theor **44**, 492002 (2011).

[37] A. Levy and R. Kosloff, Quantum absorption refrigerator, Phys. Rev. Lett. **108**, 070604 (2012).

[38] N. Brunner, M. Huber, N. Linden, S. Popescu, R. Silva, and P. Skrzypczyk, Entanglement enhances cooling in microscopic quantum refrigerators, Phys. Rev. E **89**, 032115 (2014).

[39] L. A. Correa, J. P. Palao, D. Alonso, and G. Adesso, Quantum-enhanced absorption refrigerators, Scientific Reports **4**, 3949 (2014).

[40] J. B. Brask and N. Brunner, Small quantum absorption refrigerator in the transient regime: Time scales, enhanced cooling, and entanglement, Phys. Rev. E **92**, 062101 (2015).

[41] J. Wang, Y. Lai, Z. Ye, J. He, Y. Ma, and Q. Liao, Four-level refrigerator driven by photons, Phys. Rev. E **91**, 050102 (2015).

[42] M. T. Mitchison, M. P. Woods, J. Prior, and M. Huber, Coherence-assisted single-shot cooling by quantum absorption refrigerators, New J. Phys. **17**, 115013 (2015).

[43] A. Mu, B. K. Agarwalla, G. Schaller, and D. Segal, Qubit absorption refrigerator at strong coupling, New J. Phys. **19**, 123034 (2017).

[44] S. Nimmrichter, J. Dai, A. Roulet, and V. Scarani, Quantum and classical dynamics of a three-mode absorption refrigerator,

Quantum **1**, 37 (2017).
[45] C. Mukhopadhyay, A. Misra, S. Bhattacharya, and A. K. Pati, Quantum speed limit constraints on a nanoscale autonomous refrigerator, Phys. Rev. E **97**, 062116 (2018).
[46] M. T. Mitchison, Quantum thermal absorption machines: refrigerators, engines and clocks, Contemporary Physics **60**, 164–187 (2019).
[47] S. Das, A. Misra, A. K. Pal, A. Sen(De), and U. Sen, Necessarily transient quantum refrigerator, Europhysics Letters **125**, 20007 (2019).
[48] A. Hewgill, J. O. González, J. P. Palao, D. Alonso, A. Ferraro, and G. De Chiara, Three-qubit refrigerator with two-body interactions, Phys. Rev. E **101**, 012109 (2020).
[49] A. Ghoshal, S. Das, A. K. Pal, A. Sen(De), and U. Sen, Three qubits in less than three baths: Beyond two-body system-bath interactions in quantum refrigerators, Phys. Rev. A **104**, 042208 (2021).
[50] T. Ray, S. Mondal, A. Bhattacharyya, A. Ghoshal, D. Rakshit, and U. Sen, Kerr-type nonlinear baths enhance cooling in quantum refrigerators, arXiv:2311.10499 (2023).
[51] A. Bhattacharyya, A. Ghoshal, and U. Sen, Transient effects in quantum refrigerators with finite environments, Phys. Rev. A **111**, 012209 (2025).
[52] S. Mondkar, A. Bhattacharyya, and U. Sen, Quantum refrigerator embedded in spin-star environments: Scalings of temperature and refrigeration time, arXiv:2505.04374 (2025).
[53] K. Huang, C. Xi, X. Long, H. Liu, Y.-a. Fan, X. Wang, Y. Zheng, Y. Feng, X. Nie, and D. Lu, Experimental realization of self-contained quantum refrigeration, Phys. Rev. Lett. **132**, 210403 (2024).
[54] G. Maslennikov, S. Ding, R. Hablützel, J. Gan, A. Roulet, S. Nimmrichter, J. Dai, V. Scarani, and D. Matsukevich, Quantum absorption refrigerator with trapped ions, Nat Commun **10** (2019).
[55] J.-s. Yan and J. Jing, External-level assisted cooling by measurement, Phys. Rev. A **104**, 063105 (2021).
[56] J.-s. Yan and J. Jing, Simultaneous cooling by measuring one ancillary system, Phys. Rev. A **105**, 052607 (2022).
[57] T. K. Konar, S. Ghosh, and A. Sen(De), Refrigeration via purification through repeated measurements, Phys. Rev. A **106**, 022616 (2022).
[58] D. Ghosh, T. K. Konar, and A. S. De, Measurement-based qudit quantum refrigerator with subspace cooling, arXiv:2409.08375 (2024).
[59] N. Brunner, N. Linden, S. Popescu, and P. Skrzypczyk, Virtual qubits, virtual temperatures, and the foundations of thermodynamics, Phys. Rev. E **85**, 051117 (2012).
[60] M. Ghanavati and H. Movahhedian, Self-contained n-qubit quantum refrigerator, International Journal of Quantum Information **12**, 1450018 (2014).
[61] T. K. Konar, S. Ghosh, A. K. Pal, and A. Sen(De), Designing refrigerators in higher dimensions using quantum spin models, Phys. Rev. A **107**, 032602 (2023).
[62] J. G. Krishnan, C. B. Pushpan, and A. K. Pal, Simultaneous cooling of qubits via a quantum absorption refrigerator and beyond, arXiv:2410.15871 (2024).
[63] B.-q. Guo, T. Liu, and C.-s. Yu, Quantum thermal transistor based on qubit-qutrit coupling, Phys. Rev. E **98**, 022118 (2018).
[64] H. P. Breuer and F. Petruccione, *The theory of open quantum systems* (Oxford University Press, Great Clarendon Street, 2002).
[65] M. A. Nielsen and I. L. Chuang, *Quantum Computation and Quantum Information: 10th Anniversary Edition* (Cambridge University Press, 2011).
[66] A. Rivas and S. F. Huelga, *Open quantum systems*, Vol. 10 (Springer, 2012).
[67] I. Medina, O. Culhane, F. C. Binder, G. T. Landi, and J. Goold, Anomalous discharging of quantum batteries: The ergotropic mpemba effect, Phys. Rev. Lett. **134**, 220402 (2025).
[68] D. Liu, J. Yuan, H. Ruan, Y. Xu, S. Luo, J. He, X. He, Y. Ma, and J. Wang, Speeding up quantum heat engines by the mpemba effect, Phys. Rev. A **110**, 042218 (2024).
[69] M. E. Edo and L.-A. Wu, Study on quantum thermalization from thermal initial states in a superconducting quantum computer, arXiv:2403.14630 (2024).
[70] F. Campaioli, J. H. Cole, and H. Hapuarachchi, Quantum master equations: Tips and tricks for quantum optics, quantum computing, and beyond, PRX Quantum **5**, 020202 (2024).
[71] S. G. Johnson, The NLopt nonlinear-optimization package, `https://github.com/stevengj/nlopt` (2007).